Does MPTP intoxication in mice induce metabolite changes in the nucleus accumbens? A 1H nuclear MRS study

Carine Chassain, Guy Bielicki, Carole Carcenac, Anne-Claire Ronsin, Jean-Pierre Renou, Marc Savasta, Franck Durif

Does MPTP intoxication in mice induce metabolite changes in the nucleus accumbens ? A ^{1}H nuclear magnetic resonance spectroscopy study

Carine Chassain[1,4], Guy Bielicki[2], Carole Carcenac[3], Anne-Claire Ronsin[4], Jean-Pierre Renou[2], Marc Savasta[3], Franck Durif[1,4].

[1] CHU Clermont-Ferrand, Service of Neurology, F-63001 Clermont-Ferrand, France.

[2] INRA, Centre Clermont-Ferrand/Theix, platform RMSB, F-63122 Saint Genès Champanelle, France.

[3] INSERM U836, Dynamic and Pathophysiology of Basal Ganglia, Grenoble Institute of Neurosciences, BP 170, F-38042 Grenoble, Cedex 9, France.

[4] Univ Clermont 1, UFR Medicine, EA 7980, F-63001 Clermont-Ferrand, France.

***** Running title: *A severe DA denervation in VTA induces metabolite changes in the NAc*

To whom correspondence should be addressed: Carine Chassain, CHU Clermont-Ferrand, Service of Neurology, 58 rue Montalembert, F-63001 Clermont-Ferrand, France; Tel.: +33 4 73 62 48 13; Fax: +33 4 73 62 40 89; Email: carine.chassain@clermont.inra.fr

number of pages: 37; number of figures: 9
number of words: in abstract: 266; in introduction: 556; discussion: 1569.

1

ABSTRACT

Using *in vivo* ^{1}H NMR spectroscopy in a mouse model of Parkinson's disease, we previously showed, that glutamate concentrations in the dorsal striatum were highest after dopamine denervation associated with an increase in GABA and glutamine levels. The aim of this study was to determine whether the changes previously observed in the motor part of the striatum were reproduced in a ventral part of the striatum, the nucleus accumbens (NAc). This study was carried out on controls and MPTP-intoxicated mice. *In vivo* spectra were acquired for a voxel (8 µl) in the dorsal striatum, and in the NAc (1.56 µl). NMR acquisitions were first performed 10 days after the last MPTP injection in basal condition (after saline i.p. injection) and then in the same animal the week after basal NMR acquisitions, after acute levodopa administration (200mg.kg^{-1}, i.p.). Immunohistochemistry was used to determine the levels of glutamate, glutamine synthetase (GS) and GAD67 in these two structures.

The glutamate, glutamine and GABA concentrations obtained in the basal state were higher in the NAc of MPTP-intoxicated mice which have the higher dopamine denervation in the ventral tegmental area (VTA) and in the dorsal striatum. Levodopa decreased the levels of these metabolites in MPTP-intoxicated mice to levels similar to those in controls. In parallel immunohistochemical staining showed that glutamate, GS and GAD67–immunoreactivity increased in the dorsal striatum of MPTP-intoxicated mice and in NAc for animals with a severe dopamine denervation in VTA.

These findings strongly supported a hyperactivity of the glutamatergic cortico-striatal pathway and changes in glial activity when the dopaminergic denervation in the VTA and SNc was severe.

Keywords: MPTP-intoxicated mice, ^{1}H NMR spectroscopy, Glu, Gln, GABA, dorsal striatum, NAc

INTRODUCTION

Parkinson's disease (PD) is a progressive neurodegenerative disorder characterized by a severe loss of dopaminergic neurons (DA neurons) close to 80% in the ventral part of the midbrain corresponding principally to the substantia nigra pars compacta (SNc) (1,2). Dopamine denervation is less severe (40 %), in the dorsal SNc and the contiguous ventral tegmental area (VTA) which belongs to the dorsal part of the midbrain (3-5). These nuclei project to the ventral striatum, which includes the nucleus accumbens (NAc) and the broad continuum between the caudate nucleus and the putamen ventral to the rostral internal capsule, the limbic cortex (medial prefrontal, cingulate and entorhinal areas) and other limbic structures (septum, olfactory tubercle, amygdalus, hippocampus, pyriform cortex) (6). Degeneration of the DA neurons in the SNc causes a large concomitant decrease in dopamine levels within the dorsolateral striatum (2). This part of the striatum is connected to the premotor and motor cortices areas (7,8). Using ^{1}H NMR spectroscopy to measured the levels of GABA and glutamate (Glu) in the dorsal striatum, we previously demonstrated significant increased Glu and GABA concentrations in 1-methyl-4-phenyl-1,2,3,6-tetrahydropyridine (MPTP)-intoxicated C57Bl/6J mice (9,10). MPTP is a known neurotoxin which affects primarily (though not exclusively) the dopamine-containing neurons of the SNc. It has subsequently been used to establish a mice model of PD (11). Thus, our studies strongly suggest that the motor glutamatergic cortico-striatal pathway displays hyperactivity after MPTP intoxication accompanied by an increase in striatal GABA levels. DA denervation of the VTA induces a decrease in dopamine levels within the NAc depending on the size of the VTA lesion (12-14). Damage to the mesocorticolimbic DA pathway may contribute to the non- motor symptoms described during the progression of PD, such as apathy (15) and depression (16-18). However, the consequences of DA denervation in the VTA for Glu and GABA levels in the NAc remain unclear. Only one study has shown an increase in levels of the mRNA for isoform 67 of glutamic acid decarboxylase (GAD67), an enzyme involved in GABA-synthesis, in the anterior part and core of the NAc after DA denervation (19). These results suggest that dopamine exerts a tonic inhibitory control over GAD67 mRNA synthesis in the NAc, in normal conditions.

The objective of this study was to assess the consequences of DA denervation of the VTA and the SNc after MPTP intoxication in mice for the glutamatergic and GABAergic activities in the two target structures, the NAc and the dorsal striatum. *In vivo* ^{1}H NMR spectroscopy was used to determine the levels of Glu, GABA and Gln in the NAc and the dorsal striatum of the MPTP-intoxicated mouse model of PD before and after DA replacement (intraperitoneal i.p. injection of the precursor of the dopamine, the levodopa). The concentrations obtained in the NAc were compared with the concentrations of Glu, GABA and Gln found in the dorsal striatum. We have chosen MRS due to its ability to make repeated direct non-invasive measurements of brain metabolites *in vivo*. Measurement of these metabolites concentrations using ^{1}H MRS is one way to assess Glu and GABA neurotransmitters release and glial-neuronal interactions (20,21). We also used immunohistochemistry to determine the levels in the dorsal striatum and the NAc t of Glu, glutamine synthetase (GS), an ubiquitous enzyme present in the astroglial cytoplasm and involved in the conversion of Glu to Gln (22), and GAD67.

EXPERIMENTAL PROCEDURES

Animals - All experiments were performed according to procedures conforming to European legislative, administrative and statutory regulations governing the protection of animals used for experimentation or other scientific purposes (86/609/EEC). The study design was approved by the Regional Experimental Care and Use Committee (Auvergne CREEA). The permit number for this study was CE 8-06.

We used male C57Bl/6J (Charles River, L'Arbresle, France) mice aged seven weeks and weighing 19 to 20g at the start of experiment. They were housed at 20-22°C under a 12-hour light/12-hour dark cycle.

Four control mice were used for specific localization of the NAc, with the aim of positioning the voxel of interest (VOI) precisely on MR images for NMR spectroscopy acquisitions. These mice were anesthetized and fitted with a cannula (outer diameter=0.23mm and length=4.5mm) implanted

unilaterally at the stereotaxic coordinates of the NAc, defined as in the Paxinos and Franklin (23) mouse brain atlas (coordinates with respect to bregma: A: +1.5 mm, L=0.9 mm, V=-4.0 mm). One week after surgery, MR images were acquired to visualize the trace left by the cannulae, to define anatomical landmarks and thus to localize the NAc precisely, to ensure the reproducible positioning of the VOI in the NAc.

Forty mice received i.p. injections, once daily, at 2.00 pm, for five days, of saline (0.1 ml) (20 saline-treated mice, controls) or an equivalent volume of 25 $mg.kg^{-1}$ 1-methyl-4-phenyl-1,2,3,6-tetrahydropyridine (MPTP; Sigma-Aldrich, St Louis, MO, USA) in saline (20 MPTP-intoxicated mice), as previously described (9,24). From them, twenty mice (10 controls and 10 MPTP-intoxicated mice) were assessed by behavioral tests and the other twenty mice were used for ^{1}H NMR spectroscopy and immunohistochemistry analysis.

Behavior - All behavior tests were carried out between 8.00 am and 1.00 pm, for both groups of animals. The rotarod (25,26) and pole tests (26,27) were started the morning before the first saline or MPTP injection (d-5) and were performed three days (d3) and ten days (d10) after the last injection (fig 1). On d10, animals were tested 60 minutes after the i.p. administration of saline (0.2 ml) and the following day (d11), 60 minutes after levodopa/benserazide i.p. administration at the dose that we previously used: 200 $mg.kg^{-1}$/75 $mg.kg^{-1}$ in 0.2 ml saline (10).

Rotarod test - The animals were positioned on the rotarod (TSE systems GmbH, Bad Homburg, Germany). The rotarod was programmed to rotate such that its speed increased linearly from 4 to 40 rpm in 300 seconds. An automatic sensor was used to determine the point at which the animals fell off the rod and to calculate the total time, in seconds, spent on the rod. On the days of testing, mice were trained to stay on the rod during three 60 s sessions, separated by intervals of 10 minutes. The rod did not turn at all during the first training session, and it turned at a fixed of 4 rpm in the two next. The test phase started 30 minutes later and consisted of four successive trials separated by 15-minute inter-trial intervals. The mean total time spent on the rod in the four trials was determined and is given together with the standard deviation (SD) for each group.

Pole test - The pole test involved the use of a 50 cm high wooden pole, 0.5 cm in diameter, wrapped in gauze to prevent slipping and positioned with the base in the home cage (26,27). An eraser was glued on top of the pole to help position the animals on the pole. The time at which the animal turned nose down (T_{turn} in s) and the total time required to climb down the pole (locomotion activity time, T_{LA} in s) were measured, with a maximum value of 120 s. If the mouse failed to turn nose down and instead dropped from the pole, T_{LA} was taken as 120 s (the default value), because this was assumed to indicate the maximal severity. During testing sessions at d-5, d3 and d10, each animal underwent three successive trials, with a five-minute interval between trials. The data presented are the scores obtained during the third trial and are expressed as the mean ± SD for each group of animals.

In vivo ^{1}H NMR spectroscopy - *In vivo* NMR spectra were acquired at 9.4 T, on a Bruker Avance DRX 400 micro-imaging system with a wide-bore vertical magnet and an actively shielded gradient coil (Bruker, Ettlingen, Germany). The animals were assessed between 10 and 17 days after the last MPTP or saline injection (fig 1: d10 to d17) and NMR spectra were acquired after saline administration (0.2 ml; i.p.). To assess the impact of levodopa administration on the metabolites amounts, one week later each animal was assessed again (fig 1: d17 to d24) after levodopa/benserazide administration (i.p.; 200 $mg.kg^{-1}$/75 $mg.kg^{-1}$ in 0.2 ml saline). The animals were anesthetized by spontaneous inhalation, through a mask, of 1-2.4 % isoflurane and air (300 $ml.min^{-1}$). They were carefully secured in a Bruker MicroMouse 2.5 animal handling system with their heads positioned in the center of a 20 mm diameter birdcage radiofrequency coil for excitation and signal reception. The air temperature surrounding the mouse chamber was maintained at 39°C by the circulation of warm air, under the control of a heat sensor. The mice breathed freely during the NMR acquisition and the concentration of anesthetic was adjusted to maintain respiratory rate close to 80 bpm.

The positions of the VOIs were determined on T_2-weighted images (a single-shot multi echo -RARE sequence- echo time 36 ms, recycling time 4.5 s, 19 slices 0.8 mm thick) in accordance with data from the Paxinos and Franklin atlas (23). The dorsal striatum VOI was 8 µl (2×2×2 mm) in size. The position of the NAc VOI was determined from anatomical landmarks defined by viewing the trace left

by the cannula on the magnetic resonance images in relation with the mouse brain atlas. The anatomical landmarks were the end of the lateral ventricle and the anterior part of the anterior commissure. The NAc VOI was 1.56 µl (1.16×1.16×1.16 mm) in size. NMR spectra were obtained for both structures, for each animal. All first- and second-order shim terms were manually adjusted for the VOIs. Generally, a half-height linewidth of the water signal of 12 Hz was achieved in the dorsal striatum. The linewidth of the water signal was around 15 Hz in the NAc voxel. A point-resolved spectroscopy sequence (PRESS) was used for located signal acquisition (TE = 8.8 ms; TR = 4000 ms; spectral width = 5000 Hz). The water signal from the VOIs was suppressed by variable-power RF pulses with optimized relaxation delays (VAPOR) (28). Each spectrum acquired for the dorsal striatum corresponded to a mean of 512 scans whereas each spectrum acquired for the NAc corresponded to a mean of 1024 scans. A spectrum was acquired in the same conditions without VAPOR water suppression for the absolute quantification of metabolites. For brain ^{1}H NMR spectroscopy, resonances of low-molecular weight metabolites, such as lactate (Lac), N-acetyl aspartate (NAA), total creatine (creatine and phosphocreatine; tCr), total choline (glycerophosphocholine and choline; tCho), glutamate + glutamine (Glx) and myo-inositol (Myo-Ins) overlapped with those of macromolecules (proteins and lipids). To minimize the contribution of macromolecules to the absolute quantification of the metabolites, we acquired a macromolecules spectrum applying the metabolite-nulling technique (29,30). A PRESS sequence was used with an extra inversion pulse. Before this study, the inversion time recovery (TI) was adjusted to nullify the metabolite signal in the dorsal striatum and NAc of four mice. A TI of 923 ms was defined.

To correct the metabolite concentration, the T_1 and T_2 relaxation times of water and NAA, tCr, tCho, Glx, Tau and Myo-Ins were calculated from spectra acquired in the two voxels, as previously published (9,10). Each spectrum corresponded to a mean of 4 or 128 scans for water and metabolites T_1 and T_2 determinations, respectively. Signals were acquired with an echo time of 8.8 ms and five different recycling times ($TR_{1\text{-}5}$ = 1000/2000/4000/8000/10000 ms) for longitudinal relaxation time (T_1) measurements and with TR=4000 ms and 10 different echo times ($TE_{1\text{-}10}$ =

8.8/20/30/40/60/80/100/130/180/250 ms) for transversal relaxation time (T_2) measurements. The relaxation times (T1 and T2) measured were in accordance with those previously published (9).

In vivo metabolite concentrations were determined from VOI spectra after subtraction of the macromolecules spectrum with jMRUI software. The quantification method used was the time-domain semi-parametric algorithm QUEST, based on signals for a basis set of simulated metabolites. This basis set of metabolites included the following nine molecules: tCr, tCho, GABA, Glu, Gln, Lac, Myo-Ins, NAA and Tau. The intensity of the water signal obtained from non- suppressed water spectra was used as an internal reference. For this purpose, we determined the brain water content for four control mice and four MPTP-intoxicated mice. Animals were killed by decapitation and their brains were quickly removed and dried in a drying oven. The percentage water content was calculated from the difference in weight between the freshly removed whole brain and its residue after dehydration. The water content of controls mouse brain was 78.6% ± 2.4%, whereas that of MPTP-intoxicated mouse brain was 79.6% ± 1.8% (values similar to published data, 9,31,32). We assumed the visibility of the water signal to be 100% and used a water molarity of 55.5M. Corrections were performed to take account of the T_2 and T_1 effects of water and metabolites, as previously described (9,10). For each metabolite, we applied the T_1 correction factor ($1/1\text{-}exp^{(-TR/T1)}$) with TR=4s and the T_2 correction factor ($1/exp^{(-TE/T2)}$) with TE=8.8 ms.

The reliability of metabolite quantification was assessed from the average Cramer-Rao lower bounds (CRLB) calculated by jMRUI. CRLB are estimates of the % SD of the fit for each metabolite (33,34). Only results with a CRLB ≤ 30% were included in the analysis. *In vivo* results are expressed in mM, as means ± SD.

Immunohistochemical labels-

Tissue preparation - Following the acquisition of NMR spectra, five controls and five MPTP-intoxicated mice chosen at random were killed 60 minutes after the i.p. injection of saline. Five controls and five MPTP-intoxicated mice, also chosen at random were killed 60 minutes after the i.p. injection of levodopa/benserazide (i.p.; 200 $mg.kg^{-1}$/75 $mg.kg^{-1}$ in 0.2 ml saline). These animals were

deeply anesthetized with sodium pentobarbital (180 $mg.kg^{-1}$; i.p.) and then transcardially perfused with 4% paraformaldehyde in 0.1 M phosphate buffer (pH 7.4). Their brains were removed, post-fixed by incubation in the same buffer for 1 h at 4°C and included in paraffin. We prepared 7 µm coronal sections from the substantia nigra (SNc) and the ventral tegmental area (VTA) for tyrosine hydroxylase (TH) immunohistochemistry, to validate the DA loss after MPTP intoxication. We also prepared 7 µm coronal sections from the dorsal striatum and the NAc for glutamate (Glu), glutamate decarboxylase (GAD) isoform GAD67 and glutamine synthetase (GS) analyses.

Immunohistochemical staining - Tissue sections were deparaffinized by incubation with xylene and were then rehydrated. Antigen retrieval was performed by bringing slides to the boil in 10 mM sodium citrate, pH 6.0, maintaining them just below boiling point for 20 minutes, and then cooling them at 20°C for 20 minutes. The sections were then washed for five minutes in distilled water and 10 minutes in wash buffer [0.1% Tween 20, 50 mM NaF in 1X Tris-buffer saline (TBS)], then incubated for 10 minutes in buffer containing 3% H_2O_2 (Peroxidase blocking solution DAKOCytomation, Carpinteria, CA, USA). They were then washed again in the wash buffer for 10 minutes. The SNc and VTA sections were incubated overnight at 4°C with a rabbit polyclonal anti-TH antibody (1:500; Chemicon International, Temecula, CA, USA). The dorsal striatum and NAc sections were incubated overnight at 4°C with a rabbit polyclonal anti-Glu antibody (1:5; Chemicon International), a mouse monoclonal anti-GAD67 antibody (1:500; Chemicon International), or a mouse monoclonal anti-GS antibody (1:300; Chemicon International). The slides were washed and treated with biotinylated secondary antibody (Kit LSAB + System-HRP, DAKOCytomation) for 30 minutes at 20°C. The slides were then washed in 0.1% Tween 20 in 1X TBS, incubated for 30 minutes at 20°C with streptavidine-HRP complex (DAKOCytomation) and washed again in 0.1% Tween 20 in 1X TBS. Diaminobenzidine substrate (DAKOCytomation) was added and the slices were incubated at 20°C. The reaction was stopped by immersing the slides in distilled water, and the slides were sealed for visualization by light microscopy.

Quantitative analysis of immunostained cells - The immunostained cells were counted automatically on recorded images, with IPS 32 software (SAMBA 2005, SAMBA Technologies, Meylan, France). For each group of animals, we show the total number of positive cells, expressed as mean ± SD.

Statistical analysis - NMR data were compared by two-way analysis of variance (ANOVA) with repeated measures for one factor (treatment: saline and levodopa). A Dunnett post-hoc test was carried out if the ANOVA was significant. Behavioral data were compared by repeated measures ANOVA, followed by a Newman-Keuls post-hoc test if the ANOVA was significant. The numbers of immunostained cells in the four groups of mice were compared in a two-way ANOVA, which was followed by a Dunnett post-hoc test if the ANOVA was significant. Analyses were performed with SAS V.8.1 statistical software (Cary, NC, USA). The concentrations of GABA, Glu and Gln in the NAc, as determined by NMR spectroscopy, are expressed as a function of the number of TH-immunoreactive cells in the VTA. Linearity was assessed by calculating the correlation coefficient r.

RESULTS

Number of dopaminergic neurons in the SNc and VTA - MPTP intoxication significantly decreased (by 85 %) the mean number of TH-immunoreactive neurons in the SNc, as shown by comparison with control values (fig 2; 66 ± 13 vs 428 ± 36 TH-immunoreactive positive cells, respectively; $p < 0.001$). Levodopa administration had no impact on the number of TH-immunoreactive neurons in the SNc of controls (428 ± 36 vs. 417 ± 54) or of MPTP-intoxicated mice (66 ± 13 vs. 63 ± 17). The mean number of TH-immunoreactive neurons in the VTA decreased by 44 % after MPTP intoxication (fig 2; 88 ± 13 TH-immunoreactive positive cells for controls vs 49 ± 10 TH-immunoreactive positive cells for MPTP-intoxicated mice; $p < 0.05$). Levodopa administration also had no effect on the number of TH-immunoreactive neurons in the VTA of controls (88 ± 13 vs 90 ± 8) or of MPTP-intoxicated mice (49 ± 10 vs 43 ± 12). DA denervation was homogeneous in the SNc, while there was a large interindividual variation of the lesion in the VTA (see below).

Behavior changes after MPTP intoxication - The performance of control and MPTP-intoxicated animals in the rotarod test (fig 3) was assessed as the total time spent on the rod, expressed in seconds. The animals in the control group spent significantly more time on the rod in the third trial session (d10) than at d-5 and d0 (d10: 164 ± 9 s vs d-5: 103 ± 10 s and vs d3: 114 ± 10 s; **p<0.01). Significantly more time was spent on the rod on d10, than on the following day, after levodopa administration (200 $mg.kg^{-1}$; i.p.) (d10: 164 ± 9 s vs d11: 127 ± 15 s; **p<0.01). Whereas controls performed significantly better in the third assessment than during the first two assessments, MPTP-intoxicated mice spent similar amounts of time on the rod at d-5, d3 and d10. Levodopa administration significantly improved rotarod performance in MPTP-intoxicated mice (d11: 157 s ± 14 s vs d10: 116 ± 9 s; **p<0.01). Thus, controls spent more time on the rod than MPTP-intoxicated mice at d10 (164 s ± 9 s vs 116 s ± 9 s; #p<0.05) but less time than MPTP-intoxicated mice on day 11, after levodopa administration (127 s ± 15 s vs 157 s ± 14 s; #p<0.05).

In the pole test, MPTP-intoxicated mice needed significantly more time to turn completely than controls at d10 (fig 4A: MPTP-intoxicated mice: 7.1 ± 2.6 s vs controls: 2.2 ± 0.4 s; ##p<0.01). Furthermore MPTP-intoxicated mice required significantly longer to turn at d10 than before MPTP injection (d10: 7.1 ± 2.6 s vs d-5: 1.9 ± 0.2 s; **p<0.01). Levodopa administration (200 $mg.kg^{-1}$; i.p.) at d11 tended to decrease the amount of time required for turning, but this difference was not significant (d10: 7.1 ± 2.6 s vs d11 (+Ldopa): 4.4 ± 1.1 s; p=0.13). The time required for the control mice to turn did not differ between the three testing sessions, but these mice tended to take longer to reach the floor after levodopa administration (200 $mg.kg^{-1}$; i.p.). At d10, MPTP-intoxicated mice required significantly longer to reach the floor than control mice (fig 4B: MPTP-intoxicated mice: 13.7 ± 2.9 s vs controls: 8.2 ± 0.9 s; #p<0.05). Furthermore, the time required for MPTP-intoxicated mice to reach the floor at d10 was significantly greater than that before MPTP injection (d10: 13.7 ± 2.9 s vs d-5: 7.6 ± 0.7 s; **p<0.01). Levodopa administration at d11 significantly decreased this time (d10: 13.7 ± 2.9 s vs d11 (+Ldopa): 9.7 ± 1.5 s; *p<0.05).

Metabolite levels in the dorsal striatum and NAc, as assessed in vivo by ^{1}H-NMR spectroscopy

- *In vivo* ^{1}H NMR spectra for the corresponding brain regions are shown in figure 5. The spectra shown in figure 5A were acquired from the dorsal striatum of a control mouse and a MPTP-intoxicated mouse after saline injection and levodopa (200 mg.kg^{-1}) administration. Those in figure 5B were from the NAc. The resulting high degree of spectral resolution permitted unequivocal signal assignment. In addition to the usual signals for NAA (2.008 ppm), tCr (3.022 ppm) and tCho (3.22 ppm), the resonances of several brain metabolites Glu (2.34 ppm), Gln (2.42 ppm), GABA (2.28 ppm), Lac (1.33 ppm), Tau (3.24-3.42 ppm) and Myo-Ins (3.48-3.52 ppm) were clearly resolved. Thus, nine brain metabolites were reliably quantified. NAA, tCr, Tau and Glu were quantified in the two brain regions with Cramer-Rao lower bounds (CRLB, defined by the jMRUI software) ≤ 12% (data not shown). Gln, GABA, tCho, Myo-Ins and Lac were quantified with CRLB between 15 and 30%.

For controls, the metabolites profile obtained for the NAc and dorsal striatum were similar in the basal state (fig 5).

The Glu, Gln and GABA concentrations obtained *in vivo* in the basal state were significantly higher in the dorsal striatum of MPTP-intoxicated mice than in that of controls (fig 6A; Glu: 19.1 ± 1.5 vs. 10.6 ± 2.3 mM, ***p < 0.001; Gln: 5.9 ± 1.6 vs. 2.6 ± 1.1 mM, *p < 0.05; GABA: 3.9 ± 0.9 vs. 2.1 ± 0.5 mM, *p < 0.05). Levodopa decreased metabolite levels in the dorsal striatum of MPTP-intoxicated mice (Glu: 19.1 ± 1.5 vs. 10.2 ± 3.4 mM, ###p < 0.001; Gln: 5.9 ± 1.6 vs. 2.5 ± 0.9 mM, #p < 0.05; GABA: 3.9 ± 0.9 vs. 2.0 ± 0.8 mM, #p < 0.05). Metabolite levels in the dorsal striatum of MPTP-intoxicated mice treated with levodopa did not differ significantly from those in the dorsal striatum of controls. DA denervation in VTA and replacement with levodopa had no effect on the mean metabolite levels the NAc (fig 6B).

While individual data for MPTP-intoxicated mice obtained in the striatum and the percentage of DA denervation of the SNc were homogeneous (fig 7A), those measured in the NAc showed that GABA, Glu and Gln levels were the higher for animals which had a severe DA denervation, which were decreased after levodopa administration (fig 7B). A DA denervation of 59% in the VTA (mean

denervation for the three animals which have the more severe DA denervation in the VTA) was necessary to induce changes in metabolites levels. Furthermore, the concentrations of GABA, Glu and Gln in the NAc were significantly and inversely correlated with the number of TH-immunoreactive neurons in the VTA (respectively $r = -0.7834$, $p<0.05$; $r = -0.9896$, $p<0.01$ and $r = -0.8403$, $p<0.05$).

GAD67, Glu and GS labeling in the dorsal striatum and NAc - Immnuohistochemical labeling of GABAergic neurons with a monoclonal GAD67 antibody revealed a high density of intensely stained neurons throughout all parts of the dorsal striatum and the NAc (fig 8A). Labeling with the anti-Glu antibody revealed the presence of a high density of Glu-positive granules in the dorsal striatum and NAc, corresponding to the intra- and extracellular pool of Glu. GS immunoreactivity was demonstrated in the cytoplasm and processes of glial cells in the two areas of the brain studied.

In the dorsal part of the striatum, MPTP intoxication increased the number GAD67-positive neurons to levels significantly higher than those for controls (fig 8B; 2883 ± 238 vs 1501 ± 64; $p<0.001$). The number of Glu-positive granules was also higher in the dorsal striatum of MPTP-intoxicated mice than controls (11455 ± 1560 vs 5399 ± 446; $p<0.01$). Furthermore, the number of GS-positive astrocytes was significantly higher in the dorsal striatum of MPTP-intoxicated mice than in that of controls (7283 ± 585 vs 3440 ± 454; $p<0.01$). Levodopa administration had no impact on the number of GAD-immunoreactive neurons, Glu-positive granules and GS-positive astrocytes in the dorsal striatum of controls and MPTP-intoxicated mice. DA denervation or replacement with levodopa had no impact on the mean number of positive neurons, granules and astrocytes in the NAc (fig 8B). However, individual data showed that GAD67, Glu and GS positive cells assessed in the NAc were higher for animals which had a severe DA denervation in the VTA (fig 9B).

DISCUSSION

This work illustrated the possibility to follow *in vivo,* using short-echo PRESS NMR localized spectroscopy, the metabolites levels in a small volume (1.56 µl) encompassing the NAc. We first showed that the metabolic profile of this structure was identical to this obtained in the dorsal striatum.

306 Secondly, the MPTP intoxication of the mice increased GABA, Glu and Gln concentrations in the
307 dorsal striatum and in the NAc showing that the DA denervation was sufficient in the VTA (>59%).
308 Thirdly, levodopa decreased metabolite levels in the dorsal striatum of MPTP-intoxicated mice and in
309 the NAc for MPTP-intoxicated animals which showed the highest levels of GABA, Glu and Gln.
310 Finally, changes in metabolites concentrations in the dorsal striatum and in the NAc were associated
311 with changes in Glu metabolism, as shown by immunohistochemistry and characterized by an increase
312 in the number of GAD67-reactive-neurons, Glu-positive granules and GS-positive astrocytes.
313
314 In this study, jMRUI fitting to the spectra acquired for the NAc yielded the same
315 neurochemical profile as obtained for the dorsal striatum. Anatomically, the NAc is a major part of the
316 ventral striatum and the cell types present are similar to those in the dorsal striatum. Indeed, 90% of
317 the neurons in the NAc are GABAergic medium spiny neurons and the axon terminals in the NAc are
318 mainly DA terminals from the VTA and glutamatergic neurons from the prefrontal cortex (35). It is
319 therefore not particularly surprising that the metabolic profiles of these two structures are similar.
320 Glu and GABA levels in the dorsal striatum, as assessed by ^{1}H NMR spectroscopy were
321 dramatically increased after MPTP intoxication. Changes were also observed in the NAc for animals
322 which had the most severe VTA denervation (>59%). In fact, change in metabolites levels in the
323 striatum depends on the severity of the dopaminergic lesion of the SNc and the VTA, which induces in
324 turn a dramatic decrease of dopamine level in the dorsal and ventral striatum. Indeed, all studies which
325 reported changes in glutamatergic cortico-striatal and GABAergic activity in the dorsal striatum have
326 been shown in animal models to display a decrease of more than 60% in the number of DA neurons in
327 SNc (9,10,36). Furthermore, Retaux *et al.* (19), showed that a bilateral total electrolytic lesion of the
328 VTA in the rat induced an increase in GAD67 mRNA levels in the anterior and core part of the NAc.
329 In our study, MPTP intoxication decreased the number of DA neurons by a mean of 85% in the SNc,
330 and 44% in the VTA which may explain why no significant change of mean metabolites levels was
331 observed in the NAc. The different profile of dopaminergic denervation in the SNc and the VTA could

be due to a specific sensivity of dopaminergic neurons to MPTP. A more severe dopaminergic denervation in the SNc than in the VTA is commonly observed in other studies using MPTP (37-39). Furthermore, in PD, highly vulnerable DA subpopulations within the SNc and their axonal projections to dorsal parts of the striatum are almost completely lost, whereas neighboring DA subpopulations within the VTA and their projections to the NAc have much higher survival rates (1,40). The dopamine deficiency is thus much greater in the dorsal striatal than in the NAc (12).

Taken together, these results suggest that changes in metabolites levels in the NAc and the dorsal striatum may be linked to the severity of DA denervation in the VTA and the SNc and could be used as marker of the severity of the disease. Other studies assessing the relationship between the severity of the dopaminergic lesion in SNc and VTA and the change in striatal metabolite levels are mandatory to confirm this hypothesis.

The increase in Glu levels observed after MPTP intoxication was consistent with the increase in the number of Glu-positive granules observed on immunohistolabeling. It confirmed our previous results (9,10) and it was in accordance with several other studies showing long-term changes in excitatory striatal inputs after dopamine depletion, such as an increase in striatal Glu release, in mean percentage of asymmetrical synapses and phosphorylation, and in the abundance of Glu receptor subunits (36,41-44). The high levels of GABA after MPTP intoxication were consistent with the increase in the number of GAD67-immunoreactive neurons in the dorsal striatum and the NAc of dopamine-depleted mice. These changes were due to an increase in the basal activity of striatal neurons following DA denervation, because GAD67 expression is considered to be an index of GABAergic striatal efferent neuron activity (45,46). And several other studies showed an increased in the electrical activity of GABAergic neurons (47), the enhanced release of GABA (48) and an increase in GAD67 mRNA levels (49).

Finally, the increase in Gln levels after MPTP intoxication was associated with higher GS immunolabeling in the dorsal striatum and in the NAc of MPTP-intoxicated mice. These results suggested that DA denervation modifies glial activity. Similarly, a recent study clearly demonstrated a

358 relationship between GLT-1, a glial high-affinity Na^+/K^+-dependent Glu transporter, and changes in
359 extracellular Glu levels in the dorsal striatum of hemi-parkinsonian rat (50). The authors showed an
360 upregulation of both the production and function of striatal GLT-1 after unilateral 6-OHDA lesioning.
361 They hypothesized that an interplay between several glial and vesicular Glu transporter families might
362 underlie abnormal glutamatergic neurotransmission in PD. There are several possible reasons for the
363 increase in glial activity in the dopamine-depleted dorsal striatum. Firstly, the DA denervation may
364 directly induce an increase in GS activity and, thus, glial hyperactivity. Secondly, the increase in Gln
365 levels in the neuronal and/or the glial in the striatum of MPTP-intoxicated mice may be related to an
366 increase in the Glu/Gln cycling and, by inference, synaptic glutamatergic transmission. Glu released
367 by glutamatergic neurons has been shown to be taken up from the synapses rapidly by glia, through
368 high-affinity Glu transporters, and converted into Gln by GS (51) Gln is subsequently released by
369 astrocytes and taken up by neuronal terminals, in which it is converted enzymatically (glutaminase)
370 back into Glu, thereby replenishing the neurotransmitter pool of Glu. This Glu/Gln cycle between
371 neurons and astrocytes predominantly reflects the rates of Glu release and reuptake, thus providing an
372 indication of synaptic glutamatergic activity (52-55).
373 The present investigation did not show changes in other amino acids absolute levels after MPTP
374 intoxication in the dorsal striatum and the NAc. Our results could be consistent with the absence of
375 neuronal death in the striatum of PD. Furthermore, abundant NAA levels in unaffected GABAergic
376 cells within the striatum may be masking its depletion, as dopaminergic nerve terminals affected by
377 MPTP represent only 9% of all synapses in the striatum (56).
378 A single challenge dose of levodopa (200 $mg.kg^{-1}$) normalizes Glu, Gln and GABA levels in
379 the dorsal striatum of MPTP-intoxicated mice, and also in the NAc for mice which had high GABA,
380 Glu and Gln levels following severe dopaminergic denervation in VTA. This high dose of levodopa
381 induced a decrease in the motor performance of controls probably related to the sedative effect of
382 levodopa (57), but we nonetheless chose to use this dose, which is known to induce behavioral
383 changes (58) and changes in levels of striatal metabolites (59) in MPTP-intoxicated mice. This high

dose of levodopa may attenuate hyperactivity of the glutamatergic cortico-striatal pathway, thereby decreasing the levels of Glu and, subsequently, Gln and GABA. Changes in Glu, Gln and GABA levels were not associated with changes in the intensity of immunolabelings performed 60 minutes after acute levodopa administration. Carta *et al.* (60) showed that, three days after priming, a single administration of levodopa yielded changes in GAD67 mRNA levels in all striatal neurons not observed in drug-naïve 6-OHDA-lesioned rats. We suggest that the short time interval between levodopa administration and immunolabelings (60 minutes) might account for the lack of change in the staining observed.

In this study, we chose to use the rotarod and pole tests to assess the motor behavior of mice. The rotarod test is widely used in the evaluation of MPTP models (61). We observed significant differences in performance between MPTP-intoxicated mice and controls. In general, the results obtained depended strongly on the dose of the toxin administered. Low and moderate MPTP doses produced no measurable impairment, whereas higher doses, such as that used here, have been shown to trigger performance deficiencies in the rotarod test (62). The pole test was used to assess the agility of the animals (27,61,62). This task involved skilled grasping by the forelimbs and maneuvering requiring the basal ganglia to be intact. The decrease in pole test performance described here was consistent with that reported in previous studies (26) and reflected a nigrostriatal dysfunction. Levodopa administration improved the rotarod performance and also the results to the pole test of MPTP-intoxicated mice. Taken together, these behavior results reflect a dysfunction of the basal ganglia that was improved by levodopa administration and thus confirms a striatal dopaminergic deficit following the dopaminergic lesion induced by MPTP in the SNc and the VTA.

In conclusion, localized ^{1}H NMR spectroscopy assessed the metabolic profile longitudinally *in vivo* according to the animal model and the therapeutic strategy in the dorsal striatum and NAc of the mice. A sufficient DA denervation in the VTA and the SNc induced increased levels of Glu, Gln and GABA in the NAc and the dorsal striatal nerve cell terminals.

ACKNOWLEDGEMENTS

This work was supported by a France Parkinson Foundation grant. The funders had no role in study design, data collection and analysis, decision to publish, or preparation of the manuscript.

REFERENCES

1. Damier P, Hirsch EC, Agid Y, Graybiel AM. The substantia nigra of the human brain. II. Patterns of loss of dopamine-containing neurons in Parkinson's disease. *Brain* 1999; **122**: 1437-1448.
2. Nagatsu T, Sawada M. Biochemistry of postmortem brains in Parkinson's disease: historical overview and future prospects. J. Neural. Transm. Suppl. 2007; **72**: 113-120.
3. Haber SN. The primate basal ganglia: parallel and integrative networks. *J. Chem. Neuroanatomy.* 2003; **26**: 317-330.
4. Liss B, Haeckel O, Wildmann J, Miki T, Seino S, Roeper J. K-ATP channels promote the differential degeneration of dopaminergic midbrain neurons. *Nat. Neurosci*. 2005; **8**: 1742-1751.
5. Lees AJ. The Parkinson chimera. *Neurology.* 2009; **72**: S2-11.
6. Fudge JL, Kunishio K, Walsh C, Richard D, Haber SN. Amygdaloid projections to ventromedial striatal subterritories in the primate. *Neuroscience.* 2002; **110**: 257-275.
7. Flaherty AW, Graybiel AM. Input-output organization of the sensorimotor striatum in the squirrel monkey. *J. Neurosci*. 1994; **14**: 599-610.
8. McFarland NR, Haber SN. Convergent inputs from thalamic motor nuclei and frontal cortical areas to the dorsal striatum in the primate. *J. Neurosci*. 2000; **20**: 3798-3813.
9. Chassain C, Bielicki G, Durand E, Lolignier S, Essafi F, Renou JP, Traore A, Durif F. Metabolic changes detected by proton magnetic resonance spectroscopy in vivo and in vitro in a murin model of Parkinson's disease, the MPTP-intoxicated mouse. *J. Neurochem*. 2008; **105**: 874-882.
10. Chassain C, Bielicki G, Keller C, Renou JP, Durif F. Metabolic changes detected in vivo by ^{1}H MRS in the MPTP-intoxicated mouse. *NMR in Biomed*. 2010; **23**: 547-563.
11. Heikkila R, Hess A, Duvoisin R. Dopaminergic neurotoxicity of 1-methyl-4phenyl-1,2,3,6-tetrahydropyridine in mice. *Science*. 1984; **224**: 1451-1453.
12. Hornykiewicz O. Biochemical aspects of Parkinson's disease. *Neurology*.1998; **51**: S2-9.
13. Cilia R, Ko JH, Cho SS, van Eimeren T, Marotta G, Pellecchia G, Pezzoli G, Antonini A, Strafella AP. Reduced dopamine transporter density in the ventral striatum of patients with Parkinson's disease and pathological gambling. *Neurobiol. of Disease*. 2010; **39**: 98-104.
14. Yagi S, Yoshikawa E, Futatsubashi M, Yokokura M, Yoshihara Y, Torizuka T, Ouchi Y. Progression from unilateral to bilateral parkinsonism in early Parkinson disease: implication of mesocortical dopamine dysfunction by PET. J Nuclear Medicine. 2010; **51**: 1250-1257.
15. Thobois S, Ardouin C, Lhommée E, Klinger H, Lagrange C, Lagrange C, Xie J, Fraix V, Coelho Braga MC, Hassani R, Kistner A, Juphard A, Seigneuret E, Chabardes S, Mertens P,

Polo G, Reilhac A, Costes N, LeBars D, Savasta M, Tremblay L, Quesada JL, Bosson JL, Benabid AL, Broussolle E, Pollak P, Krack P. Non-motor dopamine withdrawal syndrome after surgery for Parkinson's disease: predictors and underlying mesolimbic denervation.*Brain*. 2010; **133**: 1111-1127.

16. Aarsland D, Bronnick K, Alves G, Tysnes OB, Pedersen KF, Ehrt U, Larsen JP. The spectrum of neuropsychiatric symptoms in patients with early untreated Parkinson's disease. *J. Neurol. Neurosurg. Psychiatry.* 2009; **80**: 928-30.
17. Chaudhuri KR, Schapira AH. Non-motor symptoms of Parkinson's disease: dopaminergic pathophysiology and treatment. *Lancet Neurol*. 2009; **8**: 464-474.
18. Rodriguez-Oroz MC, Jahanshahi M, Krack P, Litvan I, Macias R, Bezard E, Obeso JA. Initial clinical manifestations of Parkinson's disease: features and pathophysiological mechanisms. *Lancet Neurol*. 2009; **8**: 1128-1139.
19. Retaux S, Trovero F, Besson M J. Role of dopamine in the plasticity of glutamic acid decarboxylase messenger RNA in the rat frontal cortex and the nucleus accumbens. *Eur. J. Neurosci*. 1994; **6**: 1782-1791.
20. Mangia S, Tkac I, Gruetter R, Van de Moortele PF, Maraviglia B, Ugurbil K. Sustained neuronal activation raises oxidative metabolism to a new steady-state level: evidence from ^{1}H NMR Spectroscopy in the human visual cortex. *J. Cereb. Blood Flow Metab*. 2006; **27**: 1055-1063.
21. Mangia S, Giove F, Tkac I, Logethetis NK, Henry PG, Olman CA, Maraviglia B, Di Salle F, Ugurbil K. Metabolic and hemodynamic events after changes in neuronal activity: current hypothesis, theoretical predictions and in vivo NME experimental findings. *J. Cereb. Blood Flow Metab*. 2009; **29**: 441-463.
22. Van den Berg C. Glutamate and Glutamine. Pp. 355-376 In: *Handbook of Neurochemistry* 1970; vol 3 (Lajha A, ed), New York, Plenum.
23. Paxinos G, Franklin KBJ. *The mouse brain in stereotaxic coordinates.* Academic Press. 2001. 2nd edition.
24. Monaca C, Laloux C, Jacquesson JM, Gele P, Marechal X, Bordet R, Destée A, Derambure P. Vigilance states in a parkinsonian model, the MPTP mouse.*Eur. J. Neurosci*. 2004; **20**: 2474-2478.
25. Rozas G, Labandeira Garcia JL. Drug-free evaluation of rat models of parkinsonism and nigral grafts using a new automated rotarod test. *Brain Res.* 1997; **749**: 188-199.
26. Luchtman DW, Shao D, Song C. Behavior, neurotransmitters and inflammation in three regimens of the MPTP mouse model of Parkinson's disease. *Physiol. Behav*. 2009; **98**: 130-138.

27. Ogawa N, Hirose Y, Ohara S, Ono T, Watanabe Y. A simple quantitative bradykinesia test in MPTP-treated mice. *Res. Comm. Chem. Pathol. Pharmacol*. 1985; **50**: 435-441.
28. Tkac I, Henry PG, Andersen P, Keene CD, Low WC, Gruetter R. Highly resolved in vivo ^{1}H spectroscopy of the mouse brain at 9.4T. *MRM*. 2004; **52**: 478-484.
29. Behar KL, Ogino T. Characterization of macromolecule resonances in the ^{1}H NMR spectrum of rat brain. *Magn. Reson. Med.* 1993; **30**: 38-44.
30. Pfeuffer J, Tkác I, Provencher SW, Gruetter R. Toward an in vivo neurochemical profile: quantification of 18 metabolites in short-echo-time (1)H NMR spectra of the rat brain. *J. Magn. Reson.* 1999; **141**: 104-120.
31. Agrawal HC, Davis JM, Himwich WA. Develop mental changes in mouse brain: weight, water content, and free amino acids. *J. Neurochem.* 1968; **15**: 917-923.
32. Papadopoulos MC, Manley GT, Krishna S, Verkman AS. Aquaporin-4 facilitates reabsorption of excess fluid in vasogenic brain edema. *The FASEB.* 2004; **18**: 1291-1293.
33. Provencher SW. Estimation of metabolite concentrations from localized in vivo proton NMR spectra. Magn. Reson. Med. 1993; **30**: 672-679.
34. Cavassila S, Deval S, Huegen C, van Ormondt D, Graveron-Demilly D. Cramer-Rao bounds: an evaluation tool for quantification. *NMR Biomed*. 2001; **14**: 278-283.
35. Zahm D.S. Functional-anatomical implications of the nucleus accumbens core and shell subterritories. *Ann. NY Acad. Sci.* 1999; **877**: 113-28.
36. Jonkers N, Sarre S, Ebinger G, Michotte Y. MK801 suppresses the L-DOPA-induced increase of glutamate striatum of hemi-parkinson rats. *Brain Res*. 2002; **926**: 149-155.
37. Lavoie B, Parent A, Bedard PJ. Effects of dopamine denervation on striatal peptide expression in parkinsonian monkeys. *Can J Neurol Sci.* 1991; **18**: 373-375.
38. Gnanalingham KK, Smith LA, Hunter AJ, Jenner P, Marsden CD. Alterations in striatal and extrastriatal D-1 and D-2 dopamine receptors in the MPTP-treated common marmoset: an autoradiographic study. *Synapse.* 1993; **14**: 184-194.
39. Phani s, Gonye G, Iacovitti L. VTA neurons show a potentially protective transcriptional response to MPTP. *Brain Res.* 2010; **1343**: 1-13.
40. Gonzalez-Hernandez T, Cruz-Muros I, Afonso-Oramas D, Salas-Hernandez J, Castro-Hernandez J. Vulnerability of mesostriatal dopaminergic neurons in Parkinson's disease. *Front. Neuroanat*. 2010; **4**: 140-154.
41. Anglade P, Mouatt-Prigent A, Agid Y, Hirsch E. Synaptic plasticity in the caudate nucleus of patients with Parkinson's disease. *Neurodegeneration.* 1996; **5**: 121-128.
42. Ingham CA, Hood SH, Taggart P, Arbuthnott GW. Plasticity of synapses in the rat neostriatum after unilateral lesion of the nigrostriatal dopaminergic pathway. *J. Neurosci*.

1998; **18**: 4732-4743.

43. Meshul CK, Emre N, Nakamura CM, Allen C, Donohue MK, Buckman JF. Time-dependent changes in striatal glutamate synspases following 6-hydroxydopamine lesion. *Neuroscience.* 1999; **88**: 1-16.
44. Walker RH, Koch RJ, Sweeney JE, Moore C, Meshul CK. Effects of subthalamic nucleus lesions and stimulation upon glutamate levels in the dopamine-depleted rat striatum. *NeuroReport.* 2009; **20**: 770-775.
45. Litwak J, Mercugliano M, Chesselet MF, Olman G. Increased glutamic acid decarboxylase (GAD) mRNA and GAD activity in cerebellar Purkinje cells following lesion-induced increases in cell firing. *Neurosci. Lett.* 1990; **116**: 179-183.
46. Soghomonian JJ, Martin DL. Two isoforms of glutamate decarboxylase: why? *Trends Pharmacol. Sci.* 1998; **19**: 500-505.
47. Calabresi P, Mercuri NB, Sancesario G, Bemardi G. Electrophysiology of dopamine-denervated striatal neurons. Implication for Parkinson's disease. *Brain*. 1993; **11:** 433-452.
48. Lindefors N, Brodin E, Tossman U, Segovia H, Ungerstedt U. Tissue levels and in vivo release of tachychinins and GABA in striatum and substantia nigra of rat brain after unilateral striatal dopamine denervation. *Exp. Brain. Res.* 2003; **74**: 527-534.
49. Carta AR, Fenu S, Pala P, Tronci E, Morelli M. Selective modifications in GAD67 mRNA levels in striatonigral and striatopallidal pathways correlate to dopamine agonist priming in 6-hydroxydopamine-lesioned rats. *Eur. J. Neurosci*. 2003; **18**: 2563–2572.
50. Massie A, Goursaud S, Schallier A, Vermoesen K, Meshul CK, Hermans E, Michotte Y. Time-dependent changes in GLT-1 functionning in striatum of hemi-parkinsonn rats. *Neurochem. Int*. 2010; **57**: 572-578.
51. Bergles DE, Jahr CE. Synaptic activation of glutamate transportes in hippocampla astrocytes. *Neuron.* 1997; **19**: 1297-1308.
52. Sibson NR, Dhankhar A, Mason GF, Rothman DL, Behar KL, Schulman RG. Stoichiometric coupling of brain glucose metabolism and glutamatergic neuronal activity. *Proc. Natl. Acad. Sci. USA.* 1998; **95**: 316–321.
53. Magistretti PJ, Pellerin L, Rothman DL, Shulman RG. Energy on demand. *Science.* 1999; **283**: 496–497.
54. Gruetter R. In vivo 13C NMR studies of compartmentalized cerebral carbohydrate metabolism. *Neurochem Int.* 2002; **41**: 143–154.
55. Yang J, Shen J. In vivo evidence for reduced cortical glutamate-glutamine cycling in rats treated with the antidepressant/antipanic drug phenelzine. *Neuroscience.* 2005; **135**: 927–937.

56. Groves PM, Linder JC, Young SJ. 5-hydroxydopaminelabeled dopaminergic axons: three-dimensional reconstructions of axons, synapses and postsynaptic targets in rat neostriatum. *Neuroscience.* 1994; **58**: 593–604.
57. Andreu N, Chale JJ, Senard JM, Thalamas G, Montastruc JM, Rascol O. L-Dopa-induced sedation a double-link cross-over controlled study versus trizolam and placebo in healthy volunteers. *Clinical Neuropharmacol*. 1999; **22**: 15-23.
58. Nicholas AP. Levodopa-induced hyperactivity in mice treated with 1-methyl-4-phenyl-1,2,3,6-tetrahydroxypyridine. *Mov. Disord.* 2006; **22:** 99–104.
59. Nicholas AP, Buck K, Ferger B. Effect of levodopa on striatal monoamines in mice with levodopa-induced hyperactivity. *Neurosci. Lett*. 2008; **443**: 204–208.
60. Carta AR, Fenu S, Pala P, Tronci E, Morelli M. Selective modifications in GAD67 mRNA levels in striatonigral and striatopallidal pathways correlate to dopamine agonist priming in 6-hydroxydopamine-lesioned rats. *Eur. J. Neurosci*. 2003; **18**: 2563–2572.
61. Meredith GE, Kang UJ. Behavioral models of Parkinson's disease in rodents: a new look at an old problem. *Mov Desord*. 2006; **21**: 1595-1606.
62. Tillerson JL, Caudle WM, Reveron ME, Miller GW. Detection of behavioral impairments correlated to neurochemical deficits in mice treated with moderate doses of 1-methyl-4-phenyl-1,2,3,6-tetrahydropyridine. *Exp. Neurol.* 2002; **178**: 80-90.

FIGURE 1. Experimental design.

All behavior tests were performed between 8.00 am and 1.00 pm, for both groups of animals (n=10 controls and n=10 MPTP-intoxicated mice). The first rotarod and pole tests were carried out the morning before the first saline or MPTP injection (d-5) and further tests were performed three days (d3) and ten days (d10) after the last injection. Animals were tested 60 minutes after the intraperitoneal administration of saline (0.2 ml) on d10 and 60 minutes after the administration of levodopa (200 $mg.kg^{-1}$ in 0.2 ml saline) on d11.

NMR acquisitions were performed for both other groups of animals (n=10 controls and n=10 MPTP-intoxicated mice) and begun ten days following the last MPTP injection, on d10. Spectra were acquired after the i.p. administration of saline (d10). One week later (d17), each animal was assessed again after the i.p. administration of levodopa. Animals were killed humanely once all the NMR acquisitions had been acquired (d24), 60 minutes after the i.p. administration of saline (n=5 controls and n=5 MPTP-intoxicated mice) and 60 minutes after the i.p. administration of levodopa (200 $mg.kg^{-1}$ in 0.2 ml saline; n=5 controls and n=5 MPTP-intoxicated mice).

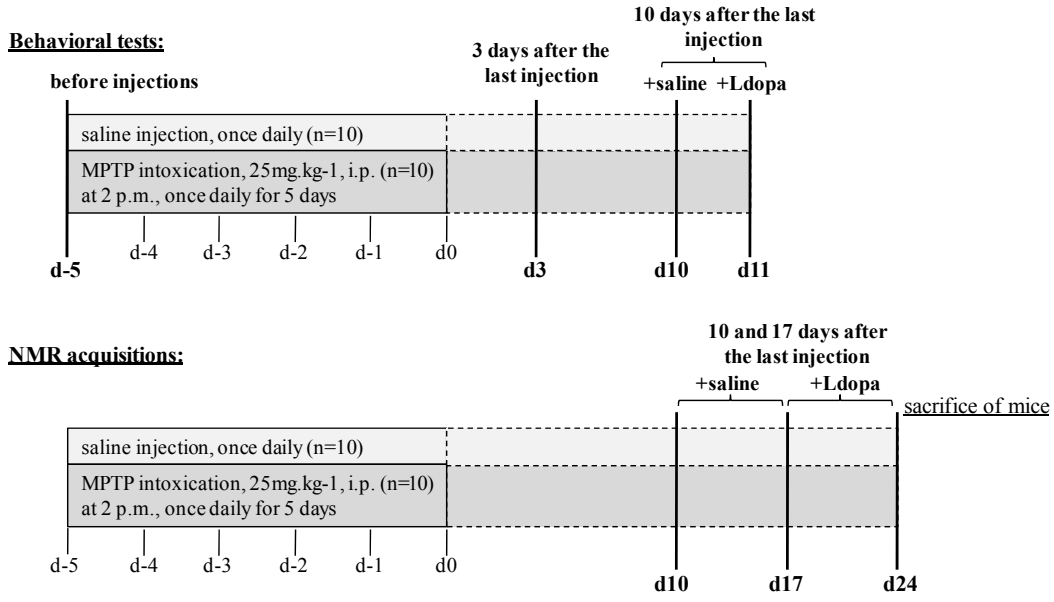

Figure 1 –

FIGURE 2. Effect of MPTP treatment on TH-immunoreactivity in SNc and VTA coronal sections.

A. Photomicrographs of representative posterior SNc and VTA sections stained with an antibody against TH. The tissues were collected 10 days after the last MPTP injection. The MPTP-intoxicated mice (5 × 25 $mg.kg^{-1}$, once daily for 5 days, i.p.) have fewer TH-positive neurons than the controls.

Scale bar, 1 mm

B. MPTP administration led to a significant decrease (85%) in the mean number of TH-immunoreactive neurons in the SNc, as shown by comparison with control values. A decrease of 44% was observed in the VTA. Means ± SD of five mice per group are presented, ***p < 0.001 and *p < 0.05 versus controls, in a two-way ANOVA followed by a Dunnett post-hoc test.

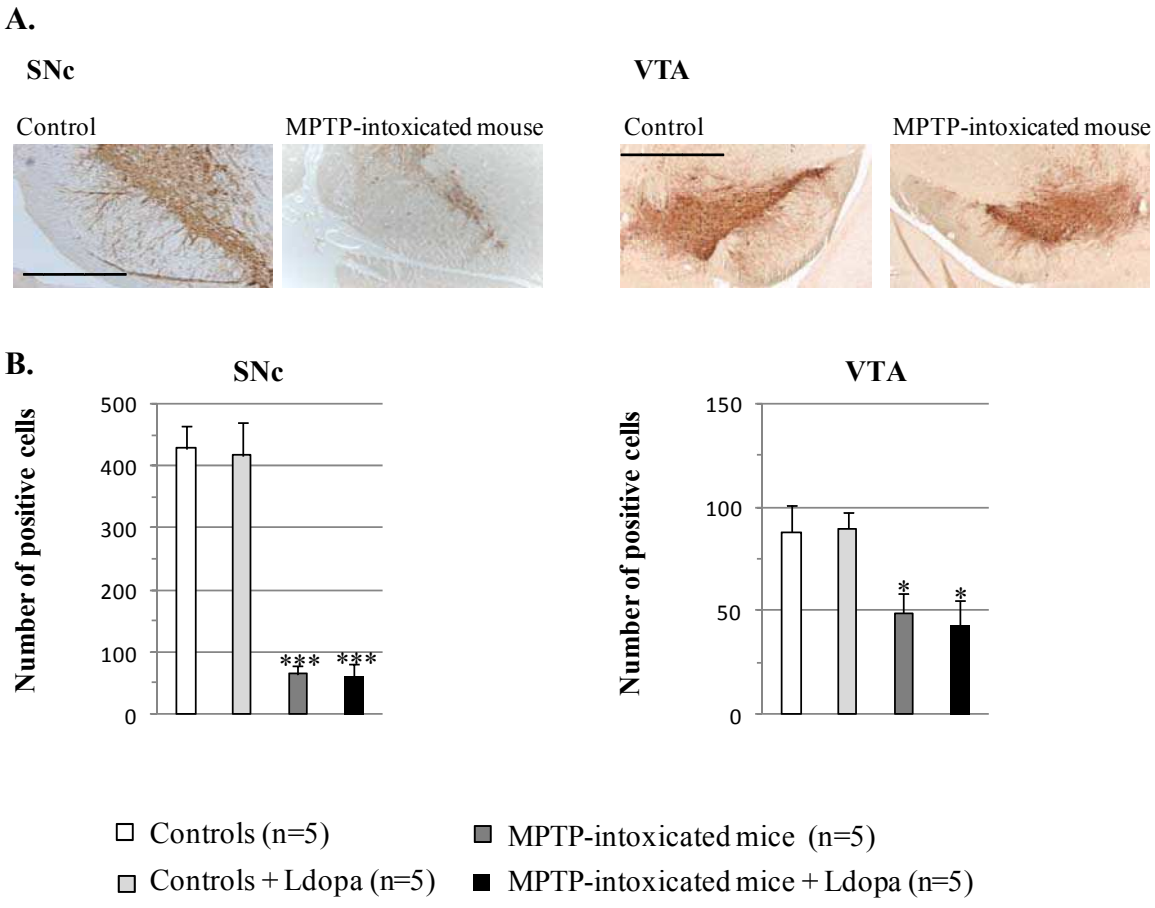

Figure 2 –

FIGURE 3. Time (s) spent on the rotarod for control mice (n=10) and MPTP-intoxicated mice (n=10).

Saline or MPTP was injected once daily for 5 days. Animals were tested on the rotarod before saline or MPTP injection (d-5), and 3 days (d3) and 10 days (d10) after the last saline or MPTP injection. On d11, they were also assessed after levodopa (200 $mg.kg^{-1}$; i.p.) administration. In the testing session, animals underwent four successive trials and the data presented are the means for these four trials. Results are presented as means ± SD (for 10 animals in each group). Within each group (controls or MPTP-intoxicated mice), asterisks (**) indicate a significant difference ($p<0.01$) with respect to the values obtained for the other trial sessions. #$p<0.05$ versus the corresponding control mean in repeated measures ANOVA followed by a Newman-Keuls post-hoc test.

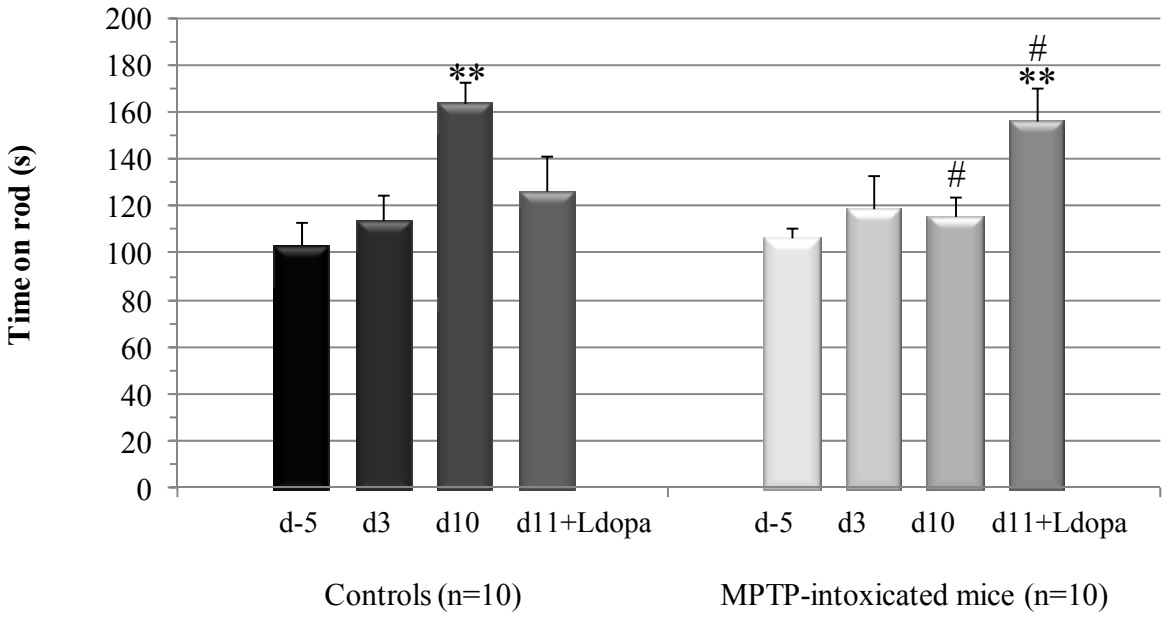

Figure 3 –

FIGURE 4. Effect of MPTP on the pole test performances.

Saline or MPTP was injected into the mice once daily for 5 days. The pole test was performed before saline or MPTP injection (d-5), 3 days (d3) and 10 days (d10) after the last saline or MPTP injection. On d11, the test was performed after levodopa (200 $mg.kg^{-1}$; i.p.) administration. A mouse was placed head upwards close to the top of a rough-surfaced pole. The times required for the animal to turn completely (T_{turn}) and to reach the floor (T_{LA}) were measured and are shown in A and in B, respectively. In the testing session, animals underwent three successive trials and the data presented are those obtained in the third trial. Results are presented as means ± SD (for 10 animals in each group).

A. T_{turn}. In the control group, the mean obtained after levodopa administration on d11 was significantly higher than the other values (*p<0.05). In the MPTP-treated group, there was a significant difference between d10 on the one hand and d-5 and d3 on the other (**p<0.01). ##p<0.01 versus the corresponding control mean in a repeated measures ANOVA followed by a Newman-Keuls post-hoc test.

B. T_{LA}. Within the MPTP-treated group, there was a significant difference between the results obtained on d10 and those obtained on d-5 and d3 (**p<0.01). There was also a significant difference between the results obtained on d10 and d11 (+Ldopa) (*p<0.05). ##p<0.01 versus the corresponding control mean in a repeated measures ANOVA followed by a Newman-Keuls post-hoc test.

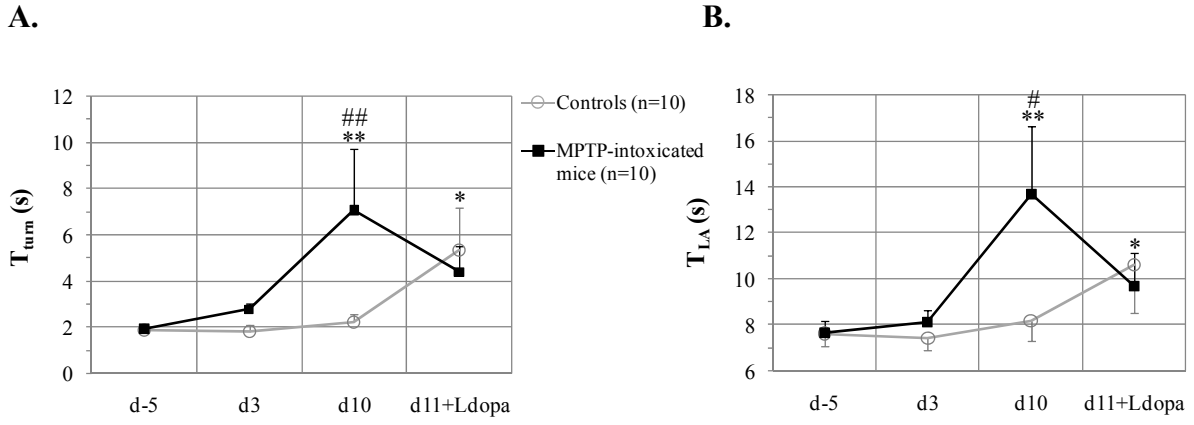

Figure 4 –

FIGURE 5. Coronal MR images of the mouse brain with the volumes of interest (VOIs) centered on the dorsal striatum (A) and NAc (B) and NMR spectra for the corresponding brain regions in a control and an MPTP-intoxicated mouse, after the administration of saline and levodopa.

The NMR images were acquired with a T_2-weighted sequence, RARE (in-plane resolution 100 × 100 µm/pixel, slice thickness 1 mm, TE = 36 ms, TR = 4.5 s).

The NMR spectra were acquired with PRESS localization, with TE = 8.8ms, TR = 4000 ms, NS = 512 for acquisition in the dorsal striatum and NS = 1024 for acquisition in the NAc; acquisition times were 34 min and 68 min respectively. Spectra were line-broadened (5 Hz), and resonances were assigned as N-acetyl aspartate (NAA) at 2.008 ppm; γ-aminobutyric acid (GABA) at 2.27 ppm, glutamate (Glu) at 2.34 ppm, glutamine (Gln) at 2.42 ppm; total creatine (tCr) at 3.022 ppm and 3.98 ppm, total choline (tCho) at 3.22 ppm; taurine (Tau) at 3.24-3.42 ppm; myoinositol (Myo-Ins) at 3.48-3.52 ppm; Glu + Gln complex (Glx) at 3.75 ppm.

A. Spectra acquired for a VOI (2.0 × 2.0 × 2.0 mm) located on the dorsal part of the striatum, for a control mouse and an MPTP-intoxicated mouse, after the administration of saline and levodopa (200 $mg.kg^{-1}$) injection.

B. Spectra acquired in a VOI (1.16 × 1.16 × 1.16 mm) located in the NAc, for a control mouse and an MPTP-intoxicated mouse, after the administration of saline and levodopa (200 $mg.kg^{-1}$) injection.

Figure 5 –

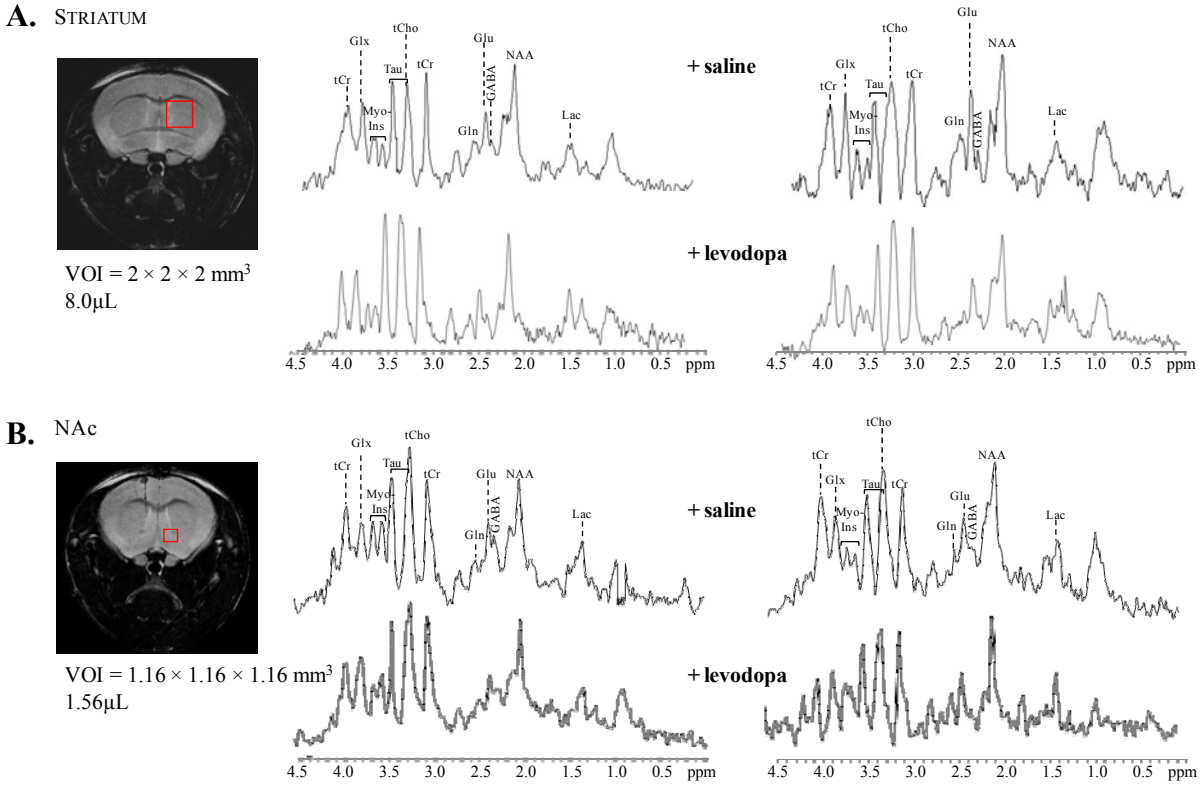
A.
STRIATUM
VOI = 2 × 2 × 2 mm3
8.0µL
+ saline
+ levodopa
B.
NAc
VOI = 1.16 × 1.16 × 1.16 mm3
1.56µL
+ saline
+ levodopa
tCr
Glx
tCho
Tau
Myo-Ins
Gln
Glu
GABA
NAA
Lac
4.5 4.0 3.5 3.0 2.5 2.0 1.5 1.0 0.5 ppm

Figure 5 –

FIGURE 6. Absolute metabolite concentrations (mM) quantified in the dorsal striatum (A) and NAc (B) of controls and MPTP-intoxicated mice, determinated by *in vivo* ^{1}H NMR after saline and levodopa administration (200 mg.kg^{-1}).

Data are the means ± SD for 10 animals in the two controls groups and 10 animals in the two MPTP-intoxicated mouse groups. Statistically significant differences are indicated for comparisons between the metabolite concentrations of controls and MPTP-intoxicated mice after the administration of saline and levodopa (200 mg.kg^{-1}), for repeated measures analysis of variance followed by a Dunnett post-hoc test. Significant differences were observed only in the dorsal part of the striatum and are indicated as: *$p < 0.05$; ***$p < 0.001$ controls + saline vs. MPTP-intoxicated mice + saline and $^{\#}p < 0.05$; $^{\#\#\#}p < 0.001$ MPTP-intoxicated mice + saline vs. MPTP-intoxicated mice + levodopa.

Figure 6 –

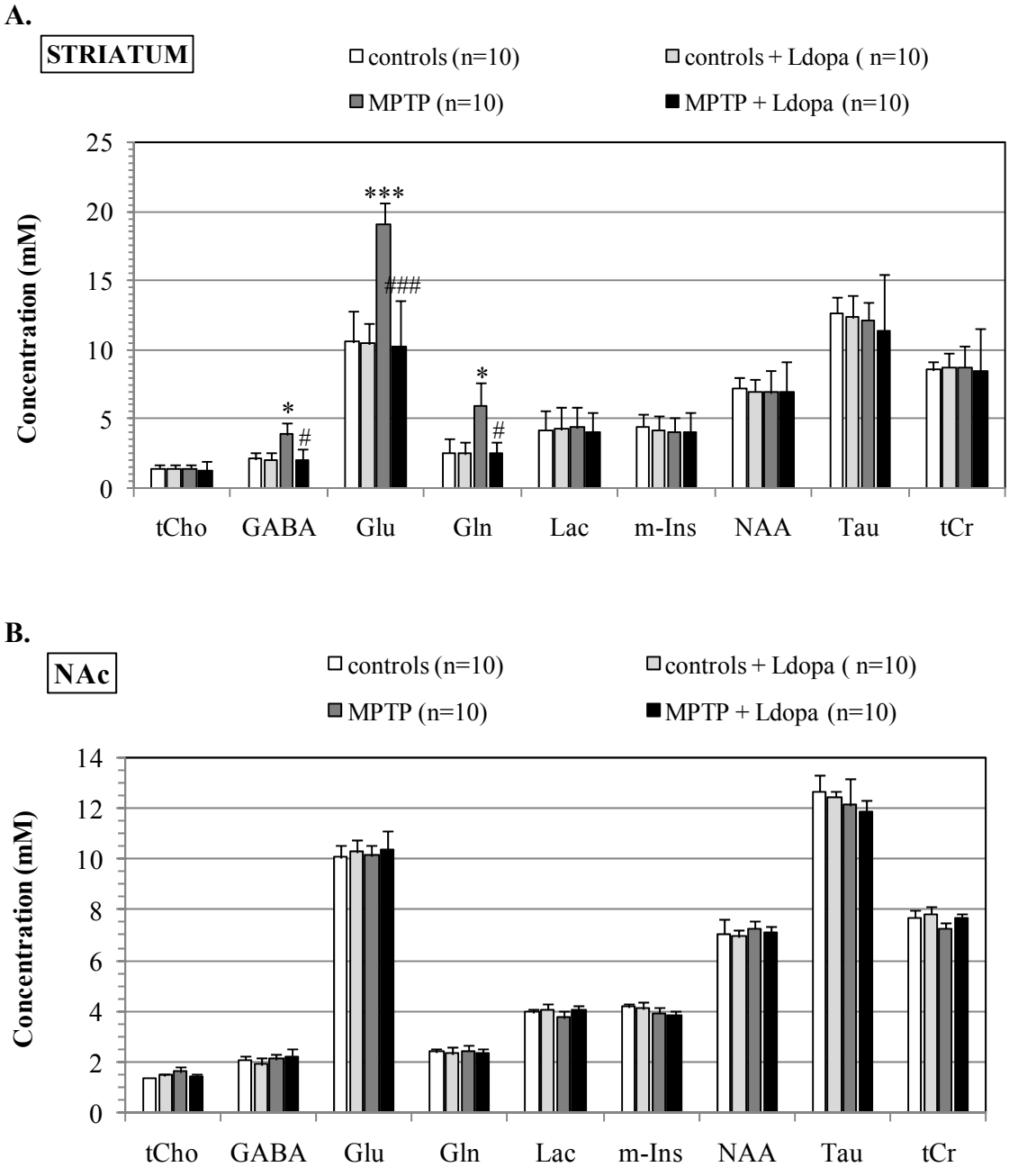
A.
STRIATUM
controls (n=10)
controls + Ldopa (n=10)
MPTP (n=10)
MPTP + Ldopa (n=10)
Concentration (mM)
25
20
15
10
5
0
***
###
*
#
*
#
tCho
GABA
Glu
Gln
Lac
m-Ins
NAA
Tau
tCr
B.
NAc
controls (n=10)
controls + Ldopa (n=10)
MPTP (n=10)
MPTP + Ldopa (n=10)
Concentration (mM)
14
12
10
8
6
4
2
0
tCho
GABA
Glu
Gln
Lac
m-Ins
NAA
Tau
tCr

Figure 6 –

FIGURE 7. Individual data measured in the dorsal striatum and the NAc in relation to DA denervation of the SNc (A) and the VTA (B), respectively.

Plotted are the GABA, Glu and Gln concentrations assessed by NMR spectroscopy in the dorsal striatum (A) and the NAc (B). Individual data points represent individual measures for the MPTP-intoxicated mice, which have been sacrified for TH immunohistochemical staining, after saline and levodopa administration (n=5). The percentages of DA denervation in the SNc and the VTA are indicated on the right.

Horizontal bars are the mean value for each group of subjects.

A.

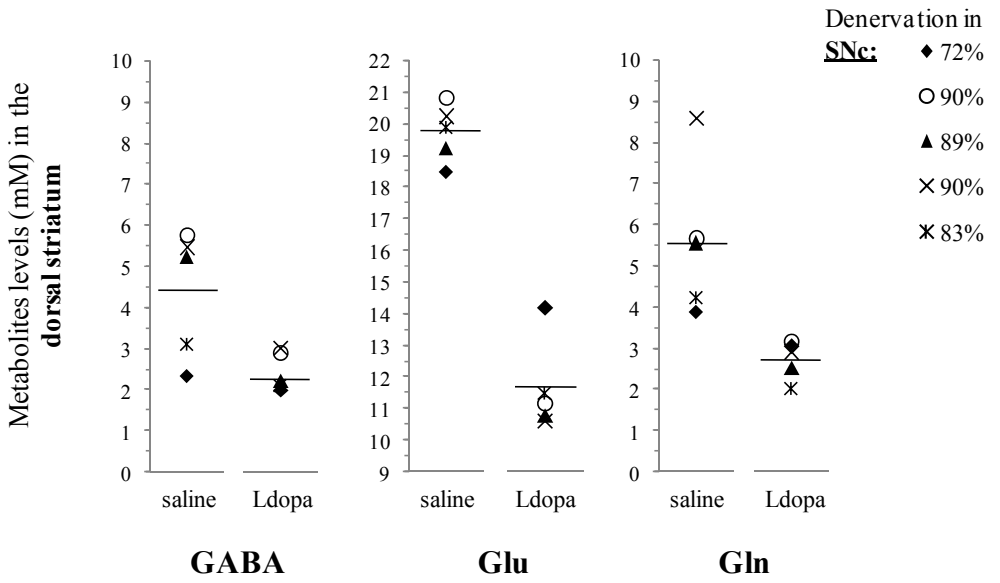
Denervation in
SNc:
72%
90%
89%
90%
83%
Metabolites levels (mM) in the
dorsal striatum
saline
Ldopa
GABA
Glu
Gln

B.

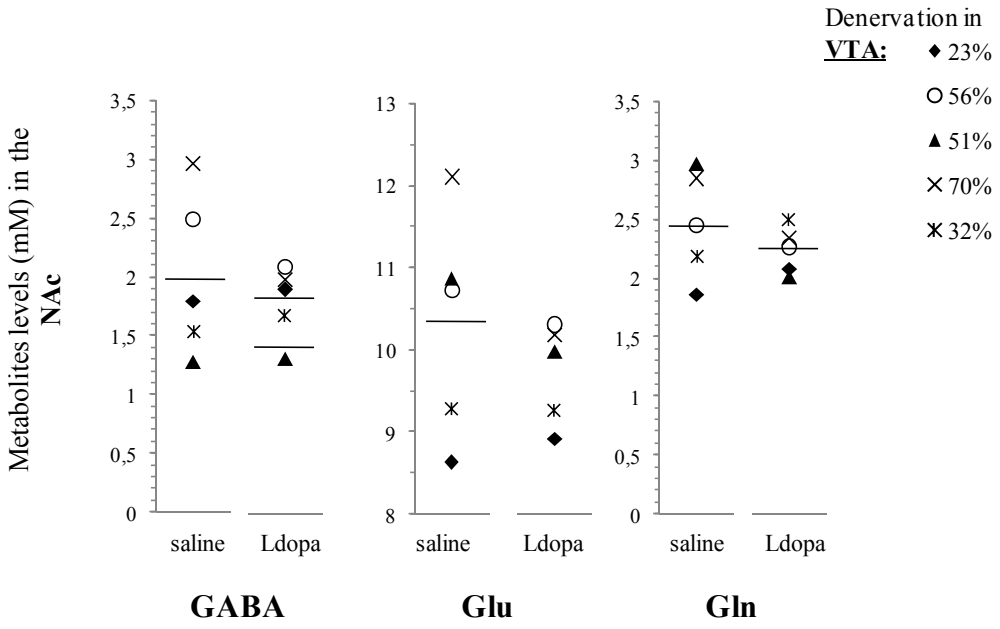
Denervation in
VTA:
23%
56%
51%
70%
32%
Metabolites levels (mM) in the
NAc
saline
Ldopa
GABA
Glu
Gln

Figure 7 –

FIGURE 8. Effect of MPTP intoxication on GAD67, Glu and GS labeling in the dorsal striatum and NAc.

A. Visualization of GAD67, Glu and GS immunolabeling in coronal slices of the dorsal part of the dorsal striatum and the NAc. The lines delimit the dorsal striatum and the area of the NAc in which immunoreactive cells were counted. Typical labeling for GAD67, Glu and GS is shown (arrows) in the insets (×20).

   Scale bar, 1 mm.

B. Quantitative analysis of the effect of DA denervation and DA replacement on the same markers in the dorsal striatum and the NAc (n=5 animals from each of the 4 experimental groups). Data are expressed as the mean number of immunoreactive cells ± SD. Statistical comparisons were performed by two-way ANOVA, followed by Dunnett's test. **$p < 0.01$ and ***$p < 0.001$ versus the control group.

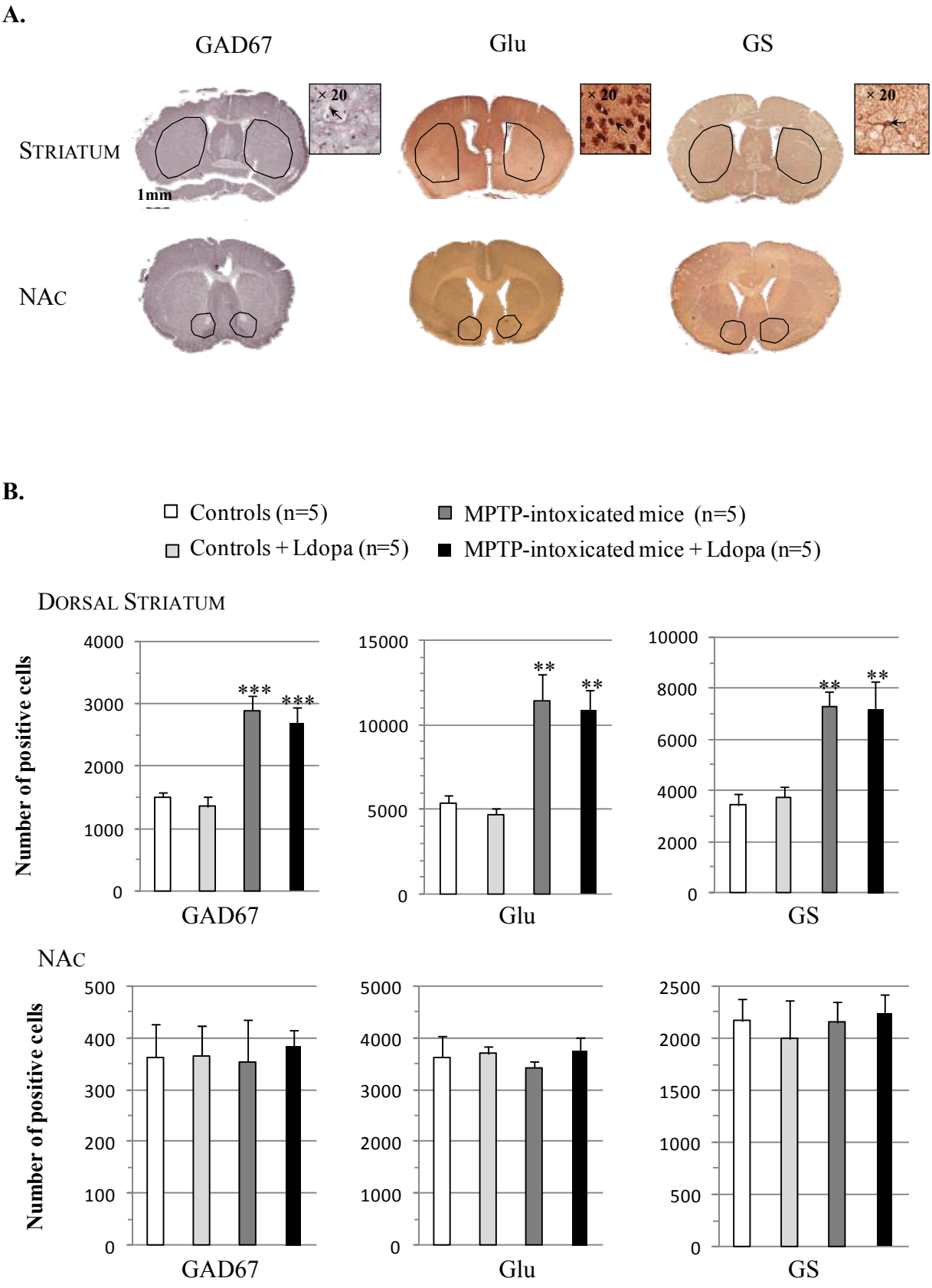
A.
GAD67
Glu
GS
STRIATUM
NAC
× 20
1mm
B.
Controls (n=5)
Controls + Ldopa (n=5)
MPTP-intoxicated mice (n=5)
MPTP-intoxicated mice + Ldopa (n=5)
DORSAL STRIATUM
Number of positive cells
GAD67
Glu
GS
NAC

Figure 8 –

FIGURE 9. Individual data measured in the dorsal striatum and the NAc in relation to DA denervation of the SNc (A) and the VTA (B), respectively.

Plotted are the immunoreactive cells counted in the dorsal striatum and the NAc. Individual data points represent individual measures for the MPTP-intoxicated mice, which have been sacrified for TH immunohistochemical staining, after saline and levodopa administration (n=5). The percentages of DA denervation in the SNc and the VTA are indicated on the right.

Horizontal bars are the mean value for each group of subjects.

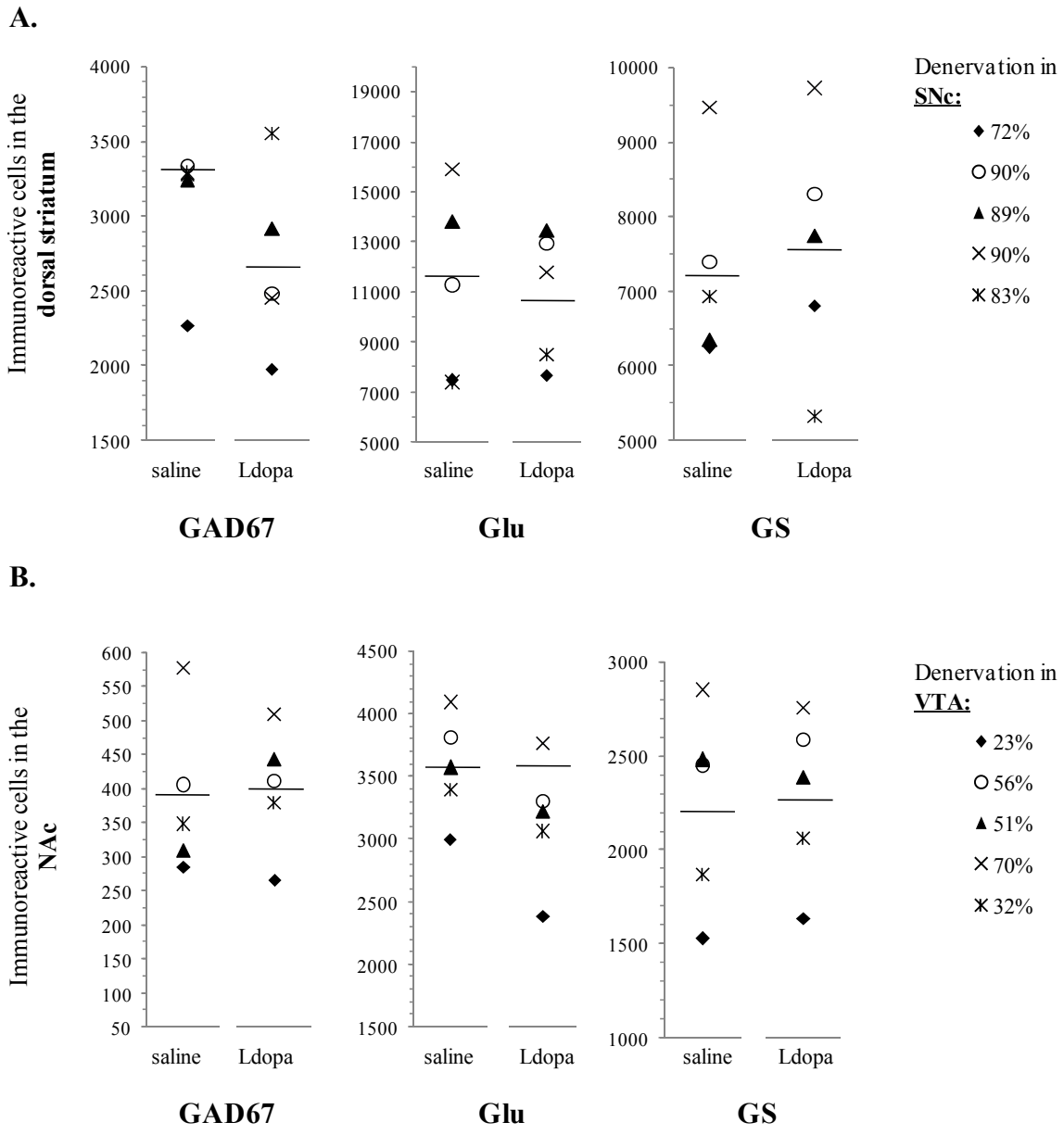

Figure 9 –